The Western Pacific Warm Pool and ENSO Asymmetry in CMIP3 Models

Yan Sun[*,1,2,3], De-Zheng Sun[3], Fan Wang[1] and Lixin Wu[2]

[1] Key Laboratory of Ocean Circulation and Waves, Institute of Oceanology, Chinese Academy of Sciences, Qingdao, China

[2] Physical Oceanography Laboratory, Ocean University of China, Qingdao, China

[3] Cooperative Institute for Research in Environmental Sciences, University of Colorado, and NOAA/Earth System Research Laboratory/Physical Sciences Division, Boulder, Colorado
USA

Submitted to AAS

July 15, 2012

[*]Corresponding author: Yan Sun, Key Laboratory of Ocean Circulation and Waves, Institute of Oceanology, Chinese Academy of Sciences (IOCAS), 7 Nanhai Road, Qingdao, 266071, China. Email: Yan.Sun.OUC@gmail.com

Abstract

Theoretical and empirical studies have suggested that an underestimate of the ENSO asymmetry may result in a climatologically smaller and warmer western Pacific warm-pool. Simulations of the tropical Pacific climate by 19 IPCC AR4 (CMIP3) climate models that do not use flux adjustment are evaluated in light of this suggestion. The evaluation reveals systematic biases in both the mean state as well as in the ENSO statistics. It is found that the mean state in most of the models has a smaller and warmer warm pool. This common bias in the mean state is accompanied by a common bias in the simulated ENSO statistics: a significantly weak asymmetry between the two phases of ENSO. Even though the too weak ENSO asymmetry and too weak or non-existent time mean effect of ENSO on the tropical mean climate are found in climate models, there are still consistent correlation evidence between warm pool simulation and ENSO asymmetry simulation based on different Niño index (Niño 3, 34 and 4), which can support our conclusion very well. Moreover, it seems that the stronger ENSO activity the climate models can simulate, the stronger ENSO asymmetry it can get. These findings add support for the suggested impact of ENSO asymmetry on the tropical mean state-the climatological size and temperature of the warm-pool in particular. More importantly, together with previous studies, the findings light up a path to improve the simulation of the tropical Pacific mean state by climate models: enhancing the asymmetry of ENSO in the climate models.

1. Introduction

While fundamentally no region in the Earth's climate system deserves special attention, the western Pacific warm-pool does have one unique aspect: it has the highest SST in the world's open oceans (Newell 1979; Ramananthan and Collins 1991). As we are increasingly concerned with whether we have reached "the point of no-return" for the earth's climate system (Hansen et al. 2008), we have good reasons to be especially concerned with our models' performance in simulating the warmest region on the Earth.

The western Pacific warm pool (here after we simply refer to as the warm-pool) has been also been referred to as a major furnace of the Earth's climate system (Pierrehumbert 1995). This is because that it is the region where tropical deep convection is concentrated and the latent heat release reaches a broad maximum (Spencer 1993). The latent heat release powers the Walker and Hadley circulation in the atmosphere, which in turn drives the currents in the upper ocean (Sun and Liu 1996; Djikstra and Neelin 1995; Trenberth and Solomon 1994; Webster and Lukas 1992; Philander 1990; Held and Hou 1980). The atmospheric Hadley circulation and its counterpart in the ocean: the meridional branch of the wind-driven circulation extends the influence of the warm pool to the extratropical region (Sun 1999; Hou1998; Lu et al. 1998). This critical role of the warm pool in dynamics of the climate system gives additional reason to know how well our state-of-the-art climate models simulate the major characteristics of the warm pool.

Some previous studies have reported some biases in the mean state of the warm pool in the coupled climate models. The earliest study using outputs from multiple models is probably the seminal one by Mechoso et al. (1995). They noted that an excessive cold-tongue was a common feature among the models they examined, implying the zonal extend of the warm pool in the models may be too confined to the west. Kiehl (1998) directly examined the warm pool simulation by CCSM1 (Kiehl et al. 1998; Boville and Gent 1998) and found the same bias as seen in Mechoso et al. (1995) in other models. Kiehl (1998) hypothesized that the excessive solar heating reaching the warm-pool may forces a stronger zonal winds and therefore an extended cold-tongue (or a smaller warm-pool). These studies, however, examined only a single run of the concerned models. As the observation is a single realization, it is important to examine the spread of the ensemble runs to draw a conclusion with confidence about the biases in the models.

We attempt to evaluate the simulations by the climate models in the fourth Intergovernmental Panel on Climate Change (IPCC) assessment report (AR4) (phase 3 of the Coupled Model Intercomparison Project (CMIP3) models) of the warm-pool and ENSO statistics in a more thorough way. We will not only examine a large set of models—we will examine all of the no flux adjustment IPCC AR4 models, but also the available ensemble runs of individual models. These ouputs allow us to construct PDFs using the largest data set available and put the estimate of bias in stronger statistical footing than studies that are limited to a single model, or to a single run of multiple models.

84 The main motivation for this study, however, is to check whether recent
85 theoretical and empirical predictions regarding a role of ENSO events in determining
86 the mean state of the warm-pool is indeed supported by, or at least consistent with the
87 results from models. Specifically, theoretical and empirical studies have suggested
88 that if models underestimate the nonlinearity in the ENSO dynamics, then the size of
89 the warm-pool should be smaller, and the mean warm pool SST is greater than the
90 observations (Rodgers et al. 2004; Schopf and Burgman 2006; Sun and Yu 2009; Sun
91 and Zhang 2006; Sun 2010). We will check whether the simulations by the climate
92 models collected by IPCC AR4 (Meehl et al. 2007) support or contradict these
93 empirical and theoretical findings. We want to check whether the way the time mean
94 state of the warm-pool is biased and the way ENSO is biased in the models have a
95 relationship that is consistent with what is implied by the aforementioned empirical
96 and theoretical results. For this purpose, we also attempt to evaluate the simulations
97 by the climate models in IPCC AR4 of ENSO statistics (ENSO asymmetry in
98 particular) in a more thorough way—in the same aforementioned manner to evaluate
99 the climatological size and temperature of the warm-pool to evaluate the statistics of
100 ENSO events. Many studies have evaluated ENSO asymmetry in climate models
101 before (An et al. 2009, Zhang et al. 2009, and Sun 2010). However, same as the
102 previous studies that have examined the climatology of the warm-pool, these studies
103 of evaluating ENSO asymmetry examined only a single run of the concerted models.
104 The number of the models examined is also more limited. For example, the study by
105 An et al. (2005) employed 10 models. The study of Zhang et al. (2009) and Sun

106 (2010) focused on the NCAR CCSMs (the early versions of CESM; see
107 http://www.cesm.ucar.edu/).

108 The collective effect of ENSO events on the mean Pacific climate in general and
109 on the warm pool in particular was first suggested from the asymmetry between its
110 warm phase (El Niño) and cold phase (La Niña)—the sum of the two does not cancel
111 but has a spatial pattern resembling the anomaly in the warm phase (Burgers and
112 Stephenson 1999, Rodgers et al. 2004, Sun and Yu 2009). This effect has been
113 referred as the residual of ENSO in these and related studies. Attempting to address
114 the questions of the time-mean effects of ENSO events more rigorously, Sun and
115 Zhang (2006) employed a hybrid model—an empirical atmosphere coupled with an
116 Ocean GCM—to contrast the response of the tropical Pacific mean climate to a
117 perturbation in the presence of ENSO events with a case in which ENSO events are
118 surgically suppressed. From the results, they found that ENSO events tend to cool the
119 center of the western Pacific warm pool and warm the central Pacific, thus effectively
120 extend the size of the warm pool but reducing mean warm pool SST. Sun (2010)
121 further reported some preliminary results from forced ocean model experiments in
122 which the strength of the ENSO fluctuations in the surface winds are varied. The
123 preliminary results seem to confirm the findings of Sun and Zhang (2006).

124 The paper is organized as follows. Information about the models and the data sets
125 is provided in section 2. The results about the biases in the climatological state of the

126 warm-pool and ENSO statistics are presented in Section 3. Summary and conclusion
127 are provided in section 4.

128 **2. Data and Methodology**

129 *2.1 Observations*

130 The observational SST data used in this study is the Hadley Centre sea ice and
131 sea surface temperature data set Version 1 (HadISST1, Rayner et al. 2003). It has
132 been developed at the Met Office Hadley Centre, and the monthly data are available
133 from 1871 to present. The SST field is built from in-situ and satellite observations and
134 is given on a 1ºx1º grid. Data used in this study cover the period from January 1900 to
135 December 1999.

136 *2.2 Models*

137 The model data are the 20c3m scenario simulations by climate models in the
138 fourth Intergovernmental Panel on Climate Change (IPCC) assessment report
139 (AR4) (phase 3 of the Coupled Model Intercomparison Project (CMIP3)
140 models) (ftp-esg.ucllnl.org (Meehl et al. 2007)). The analysis is limited to the no flux
141 adjustment models. The 19 no flux adjustment models, together with the numbers of
142 runs each individual model have in the IPCC AR4, are listed in Table 1. All together,
143 53 models runs are used in our construction of the statistics of the warm-pool
144 climatology and ENSO characteristics. The descriptions of all the models listed can
145 be obtained from this website

146 http://www-pcmdi.llnl.gov/ipcc/model_documentation/ipcc_model_documentation.p
147 hp. The whole 20th century (January 1900 to December 1999) has been employed for
148 the analysis, though we will focus on presenting the results of the last 50 years in the
149 present paper, as the observational data are more reliable during this latter period.

150 **3. Results**

151 ***3.1 Western Pacific warm pool simulation in the models***

152 The multi-model ensemble runs allow us to construct a probability density
153 function (PDF) for the warm-pool size. It is shown as the blue curve in Fig. 1a. The
154 vertical line in blue indicates the multi-model ensemble mean value-the averaged
155 warm pool size simulated by all model runs. The red line indicates the observed value.
156 The short colored bars on the horizontal axis mark the ensemble mean value of the
157 warm-pool size of each model. Fig. 1a reveals that most of the model runs have a
158 warm-pool size that is smaller than the observations. Measured by the ensemble mean
159 value of each model, ¾ of the models underestimate the size of the warm-pool. The
160 multi-model ensemble mean value of the warm-pool size is only about 80% of the
161 size of the observed warm-pool (Fig. 1a). The PDF is also obviously negatively
162 skewed, suggesting that it is more difficult to increase the size of the warm-pool in the
163 models than to decrease it.

164 Fig. 1b further shows the time series of the ensemble mean value of the
165 warm-pool size simulated by each model over the entire period where model runs are
166 available. The figure shows that the majority models that are identified to

underestimate the size of the warm-pool size do so throughout the entire century. (The few models that are identified in Fig.1a that have a larger warm-pool than in the observations do so also throughout the entire period). Redoing Fig. 1a using different periods of data show that the underestimate of the warm pool size does not depend on whether the data are from the whole 20th century, the last 50 years or the last 30 years in the 20th century are used in the construction of the PDF.

A major contributor to the smaller warm pool size in the models is that most of the models continue to have an excessive westward extension of the cold tongue (Fig. 2). The figure shows the time-mean position of the 28^{o}C SST from models and observations. The ensemble mean SST from each model is used to obtain this figure. Another contributor to the smaller size of the warm-pool is that the main part of the warm-pool (west of 160^{o}E) in the models is more confined meridionally to the equator, particularly in the northern hemisphere (Fig. 2).

The spread of the warm-pool size from different runs in the same model are found small relative to their differences with the observations. An example is given in Fig. 3 which shows the warm pool size simulated by all the runs of the same model--the NCAR CCSM3 (a) and GFDL CM2.1 (b). This suggests that the intrinsic errors in individual models are responsible for the model-observation discrepancies.

Although the size of the warm-pool in the models is generally smaller than that in the observations, the warm-pool in the models is warmer than that in the observations, measured either by the mean SST over the warm-pool (Fig. 4a,b) or its

maximum SST (Fig. 4c,d). Fig. 4 a, b and c,d are respectively the same as Fig. 1a,b except they are for the mean SST of the warm-pool (Fig. 4a,b) and for the maximum SST over the warm-pool (Fig. 4c,d). The time series of these quantities (Fig. 4b and Fig. 4d) shows that these discrepancies between the model simulations and observations remain relatively constant in the entire period of the simulations. The model-observation discrepancies in the maximum SST are particularly striking given that in the observation, the maximum SST is almost always around 30ºC –the variability is within 0.5 ºC over the entire century (Fig. 4d). The maximum SST in models spreads from 27ºC to 35ºC in comparison. 12 of the 19 models simulate a higher maximum SST. The averaged maximum SST over the tropical Indo-Pacific of all model runs is 30.85ºC, which is about 0.4ºC higher than in the observation (30.44ºC, Fig. 4c). Also note that the PDF for the maximum SST is highly positively skewed, suggesting that in the models, it is easier to increase the maximum SST than decreasing it.

This assessment reveals systematic biases in both the size and the mean temperature of the pacific Warm pool. Global coupled models tend to simulate a smaller (zonally too confined in the west and meridionally too confined in the equatorial band) and warmer western Pacific Warm Pool. This confirms the findings from previous models inter-comparison studies which diagnosed an exaggerated westward extent of the western edge of the cold tongue (and thus a Warm Pool too confined in the West) (Kug et al. 2010; AchutaRao and Sperber 2002; Davey et al. 2002; Hannachi et al. 2003; Latif et al. 2001).

3.2 ENSO asymmetry in the climate models.

Using multi-model ensemble runs, we have uncovered a common bias in the models: the warm-pool in the models is generally smaller and warmer than in the observations. This standing-out bias provides an opportunity to test the theoretical and empirical predictions about the nonlinear rectification effect of ENSO activity on the warm-pool. If the simulated ENSO statistics does have a distinct bias, and the bias is in the direction that would cause the bias we have already uncovered in the climatology of the warm-pool in the manner suggested by the aforementioned empirical studies, our suspicion of a nonlinear rectification effect of ENSO on the mean state will be enhanced. Towards this end, we have also evaluated ENSO statistics in the models, in particular, the ENSO asymmetry as it is a measure of the nonlinearity of ENSO dynamics and therefore time-mean effect (Sun and Zhang 2006; Schopf and Burgman 2006).

A typical way to measure ENSO asymmetry is the skewness of Niño3 SST (Burgers and Stephenson 1999; An et al. 2005). A PDF is constructed for the skewness of the Niño3 SST in the models and observations in the same way as for the warm-pool size and temperature. This PDF is shown in Fig 5. (The same multi-model ensemble runs are used for Fig. 5 and Fig. 1a.). The figure reveals that models generally underestimate the ENSO asymmetry. Skewness of Niño3 SST anomaly in observation is positive (redline in the Fig. 5) in contrast with the negative ones in most of the model runs (Fig. 5). Some model runs have positive skewness, but none of

them reach the observed value. The skewness of Niño3 SST anomaly from observations is 0.88 based on the 50 years data from 1950-1999. The minimum skewness of ENSO anomalies in the model runs is -0.60 and the maximum one is 0.44. The averaged skewness of Niño3 SST anomaly in all model runs is close to zero, indicating a near symmetric ENSO in the no flux adjustment IPCC models (Fig. 5).

To show this common model bias in a more traditional method, we have also plotted the histogram of the Niño3 SST anomaly distribution (Fig. 6). The symmetric nature of ENSO in the models can be readily seen from this figure. In the observations, the cooling events occurred more frequently than the warming events and the strongest cooling events are weaker than the strongest warm events. In contrast, there are equal occurrences of cooling and warming events in almost all the models. The modeled ENSO events are very near symmetric in magnitude. The modeled ENSO asymmetry biases has been noted by Leloup et al (2008) and An et al. (2009) in a more limited set of climate models. Zhang et al. (2009) noted the underestimate of the ENSO asymmetry in the NCAR CCSM models and explored its causes by contrasting the differences among the successive versions of the NCAR CCSM (and now is called CESM).

The difference in the frequency distribution of Niño3 SST anomaly among different runs by the same model is also found small relative to their differences from the observations. Fig. 7 shows the frequency distribution of monthly Niño3 SST anomaly simulated by all the runs of the same model--the GFDL models (Fig. 7ab)

255 and the NCAR models (Fig. 7cd). This suggests that the intrinsic errors in individual
256 models are responsible for the model-observation discrepancies.

257 ***3.3 Biases in the ENSO Asymmetry: A cause of a smaller and warmer warm-pool?***

258 The weak ENSO asymmetry in the models may give us an explanation of the
259 biases in the warm pool simulation in the models. As suggested by the
260 aforementioned empirical as well as theoretical studies (Rodgers et al. 2004; Sun and
261 Yu 2009; Schopf and Burgman 2006; Sun and Zhang 2006; Sun 2010), the time mean
262 effect of ENSO in the observations is to cool the center of the warm-pool, and warm
263 the central Pacific. In other words, it reduces the maximum SST over warm pool and
264 expands the warm pool size. Judging from the lack of the asymmetry in the modeled
265 ENSO, such a time mean effect of ENSO is either too weak, or non-existent in the
266 models, causing a warmer bias in the maximum SST and the mean SST over warm
267 pool, but a smaller size of the warm pool in the models.

268 Such a relationship between the warm-pool simulation and ENSO asymmetry
269 simulation in theoretical and empirical studies can be found in IPCC models but the
270 relationship is really too weak, which shows the large model biases in the state-of the
271 art climate models so far. In the IPCC AR4 models, the strong ENSO activity usually
272 means the large ENSO asymmetry in model. The left panel in Fig. 8a shows the
273 slightly positive relationship between the variance and the skewness of Niño3 SST
274 anomaly during the last 50 years of the 20th century. And there is a more slightly
275 positive relationship between the ENSO asymmetry and mean western Pacific warm
276 pool size which can be seen from the scatter plot between the mean Western Pacific

277 warm pool size and the skewness of Niño3 SST anomaly (Fig. 8b). That means in
278 IPCC models the relationship between the warm pool size and the ENSO asymmetry
279 is partially included but is also too weak. Such relationship is clear in the observation,
280 but few models can capture it. Most or near all of the models simulate too weak or
281 non-existent ENSO asymmetry and thus the weak or non-existent time mean effect of
282 ENSO. So the El Niño like residual time mean effect on the mean tropical Pacific is
283 weak in IPCC models. Although the excessive cold tongue was a common feature
284 founded by previous studies but no one linked the biases of ENSO asymmetry to
285 warm pool simulation.

286 The weak ENSO asymmetry and the resulting weak or non-existent time mean
287 effect of ENSO in models are also examined with the Empirical Orthogonal Function
288 (EOF) analysis considering the definition of the ENSO may not be accurate based on
289 the Niño3 index in models. There are 3 models (GISS_AOM, GISS_MODEL_E_H
290 and GISS_MODEL_E_R) simulate too weak or non-existent ENSO. And there are
291 two models (BCCR_BCM2_0 and CNRM_CM3) simulate stronger ENSO but very
292 small or non-existent western Pacific warm pool. Among the rest models there are
293 only two models (FGOALS_0_G and IPSL_CM4) simulate stronger ENSO than
294 observation and the rest 12 models simulate weak or much weaker ENSO than
295 observation and most of the modeled ENSO are confined to the narrow equator band
296 (Fig. 9). The modeled ENSO shows large discrepancies in both the pattern and the
297 amplitude with the observation, and also shows the weak or non-existent ENSO
298 asymmetry according to the PDF analysis of skewness of the first EOF time series in

299 models and in the observation (Fig. 10). The positive relationship between mean
300 western Pacific warm pool size and skewness is a little more distinct than the analysis
301 based on the Niño3 index, but still not so robust.

302 The weak ENSO asymmetry and weak or non-existent time mean effect of ENSO
303 in IPCC models can also be seen form the composite analysis of ENSO based on the
304 Niño3 index. Besides the 2 models that simulate too smaller or non-existent
305 warm-pool and 3 models simulate too weak or non-existent ENSO, there are 9 models
306 (csiro_mk3_5, gfdl_cm2_0, gfdl_cm2_1, ipsl_cm4, miroc3_2_hires,
307 miroc3_2_medres, ncar_ccsm3_0, ukmo_hadcm3 and ukmo_hadgem1) in the rest 12
308 models simulate the similar pattern but too weak time mean effect of ENSO (Fig. 11).
309 In observation, the western Pacific warm pool is larger, narrower and more westward
310 extended during El Niño than La Niña. Several models do simulate the larger El Niño
311 warm-pool and smaller La Niña warm-pool, which in some extent consistent with the
312 observation. But few models can capture all the features of ENSO time mean effect
313 both in pattern and amplitude. And the differences between the El Niño warm-pool
314 and the La Niña warm-pool in most of the models are too smaller than that in the
315 observations (Fig. 11). The weak or non-existent ENSO asymmetry in near all of the
316 IPCC models can contribute to the smaller and warmer western Pacific warm pool
317 simulation in some extent.

318 Niño4 and Niño34 index are also examined to evaluate the ENSO asymmetry
319 simulation in the climate models. As one aspect of the ENSO asymmetry, smaller
320 absolute value of skewness was fond in most of the models. In observation, the

skewness of Niño3 (or Niño34) is positive and the skewness of Niño4 is negative while in models the absolute value of the skewness of all the three index is small and the average of the skewness in all model runs is almost zero in all three index (Fig. 12).

Biases relationship between the warm pool simulation (size, mean SST and maximum SST) and ENSO asymmetry simulation (skewness of Niño3, Niño4 and Niño34) are also examined. The findings support our conclusions very well. The larger ENSO asymmetry biases (larger skewness biases in Niño3, Niño34 and Niño4) usually correspond to the larger biases in warm pool size (smaller warm pool), in mean SST over warm pool (lower mean SST over warm pool) and in maximum SST over warm pool (lower maximum SST over warm pool) if we just focus the quadrant the hexagrams located which means we just focus on most of the model runs not all of the model runs. That's consistent with our findings: there is a positive correlation between the biases of skewness in Niño3 (Niño34) and the biases of warm pool size while there is a negative correlation between the biases of skewness in Niño4 and the biases of warm pool size; but there is a negative correlation between the biases of mean SST (maximum SST) over warm pool and the biases of skewness in Niño3 (Niño34) while the correlation between the biases of mean SST (maximum SST) over warm pool and the biases of skewness in Niño4 is positive. **This method may not be able to give us a wholly understanding on the links between the biases in warm pool simulation and ENSO asymmetry simulation but it's certainly consistent with and can support our conclusion. (Fig. 13)**

4. Conclusions

Motivated by recent empirical as well theoretical results concerning the time-mean effect of ENSO events on the tropical Pacific climatology, we have examined the biases in the simulations of the western Pacific warm-pool in relationship with the biases in the ENSO statistics. A common bias in the simulation of the warm pool is a smaller and warmer warm pool in the models than in the observations. A corresponding common bias in the simulation of ENSO is the lack of ENSO asymmetry. Such a correspondence can be partially found in IPCC models and partially in consistent with the empirical and theoretical prediction that the underestimate of ENSO asymmetry in most of the climate models may cause a smaller but warmer warm-pool. The relationships among models are not so distinct between the warm pool simulation and ENSO asymmetry simulation since there are many factors that can affect the simulation of the warm-pool and the diversity in the models, but there are consist evidence between ENSO asymmetry biases and warm pool simulation biases among models based on there index of ENSO (Niño3, Niño34 and Niño4), the chance of such a correspondence coming out of random is likely small. It follows that the suggested time-mean effect needs to be taken seriously, and that improving ENSO statistics—the ENSO asymmetry in particular-- could be a path to improving the simulation of the tropical Pacific climatology.

It is also possible that the biases in the warm-pool climatology caused by a bias in the ENSO asymmetry may further enhance the bias in the ENSO asymmetry, causing an vicious cycle that is hard to break and thus explaining the persistence of the biases

365 that have been noted in the two key aspects of the tropical Pacific climate. Fully
366 recognizing this possibility, however, may help us to formulate a more complete
367 strategy to improve the tropical Pacific climate on which climate variability over
368 much of the world depend.

369 The importance of dynamical coupling in creating the climatological warm-pool
370 and cold-tongue configuration in the tropical Pacific has been long recognized
371 (Dijkstra and Neelin 1995; Sun and Liu 1996; Clement et al. 1996; and Jin 1996). The
372 relative roles of clouds and ocean dynamics in creating and maintaining the western
373 Pacific warm-pool have also been assessed (Clement et al. 2005). But these studies
374 have not addressed the collective role of ENSO events from the scale-interaction
375 prospective. Thus, the present study, together with those ealier ones in this line of
376 thinking (Rodger et al. 2004; Schopf and Burgman 2006; Sun and Zhang 2006; Sun
377 and Yu 2009; Sun 2010; and Liang et al. 2011) extend these theoretical and modeling
378 studies by pointing out the potential importance of rectification of ENSO events into
379 the mean in shaping the size and temperature of the warm-pool.

380

Acknowledgements

This work was supported by the Strategic Priority Research Program - Climate Change: Carbon Budget and Related Issues of the Chinese Academy of Sciences (XDA05110302), the National Basic Research Program of China for Structures, Variability and Climatic Impacts of Ocean Circulation and Warm Pool in the Tropical Pacific Ocean (2012CB417401), Chinese Scholarship Council, the Large-scale and Climate Dynamics Program of the US National Science Foundation (AGS 0553111 and AGS 0852329), the National Science Foundation for the National Science Foundation Creative Research Group Project (Grant No: 40921004). Half of the data analysis work was carried on the computers at Physical Science Division of Earth System Research Laboratory of the National Oceanic and Atmospheric Administration. We would like to thank University of Colorado at Boulder for hosting Yan Sun. We would also like to thank Dr. Tao Zhang for his help on some programming issues.

403 **References**

404 AchutaRao, K., Sperber, K.R., 2002: Simulation of the El Niño Southern Oscillation:
405 results from the Coupled Model Intercomparison Project. *Clim. Dyn.* **19**,191–209.

406 An, Soon-Il, Yoo-Geun Ham, Jong-Seong Kug, Fei-Fei Jin, In-Sik Kang, 2005: El
407 Niño–La Niña Asymmetry in the Coupled Model Intercomparison Project
408 Simulations. *J. Climate*, **18**, 2617–2627.

409 Boville, B.A., and P.R. Gent, 1998: The NCAR Climate System Model, Version one.
410 J. Climate, 11, 1115-1130. Burgers, G., and D.B. Stephenson 1999: The
411 "Normality" of El Niño, Geophys. Res. Lett., 26, 1027-1030. Clement, Amy C.,
412 Richard Seager, Raghu Murtugudde, 2005: Why Are There Tropical Warm
413 Pools?. *J. Climate*, **18,** 5294–5311. doi: 10.1175/JCLI3582.1

414 Burgers, G., and D. B. Stephenson, 1999: The "normality" of El Niño. *Geophys. Res.*
415 *Lett.*, **26,** 1027-1030, doi:10.1029/1999GL900161.

416 Clement, A. C., R. Seager, M. A. Cane and S. E. Zebiak, 1996: An ocean dynamical
417 thermostat. *J. Climate*, **9(9)**, 2190-2196.

418 Clement, A. C., R. Seager and R. Murtugudde, 2005: Why are there tropical warm
419 pools? *J. Climate*, **18(24)**, 5294-5311.

420 Davey, M., and Coauthors, 2002: STOIC: a study of coupled model climatology and
421 variability in tropical ocean regions. *Clim. Dyn.,* **18**, 403–420

422 Dijkstra, H. A., and J. D. Neelin 1995: Ocean–atmosphere interaction and the tropical
423 climatology Part II: Why the Pacific cold tongue is in the east, *J. Climate,* **8,**
424 1343–1359.

425 Hannachi, A., Stephenson, D.B., and Sperber, K.R., 2003: Probability-based
426 methods for quantifying nonlinearity in the ENSO. *Clim. Dyn.,*
427 doi:10.1007/s00382-002-0263-7.

428 Hansen, J., Mki. Sato, P. Kharecha, D. Beerling, R. Berner, V. Masson-Delmotte, M.
429 Pagani, M. Raymo, D.L. Royer, and J.C. Zachos, 2008: Target atmospheric CO_2:
430 Where should humanity aim? *Open Atmos. Sci.* J., **2**, 217-231,
431 doi:10.2174/1874282300802010217.

432 Held, I. M., and A. Y. Hou 1980: Nonlinear axially symmetric circulations in a nearly
433 inviscid atmosphere, *J. Atmos. Sci.,* **37,** 515–533.

434 Hou, A. Y. 1998: Hadley circulation as a modulator of the extratropical climate, *J.*
435 *Atmos. Sci.,* **55,** 2437–2457.

436 Hou, A. Y. 1998: Hadley circulation as a modulator of the extratropical climate, *J.*
437 *Atmos. Sci.,* **55***,* 2437–2457.

438 Jin, F.-F., 1996: Tropical ocean interaction, Pacific cold tongue, and El Niño Southern
439 Oscillation. *Science*, **274,** 76–78.

440 Kiehl, J. T. 1998: Simulation of the tropical Pacific warm-pool with the NCAR

climate system model, *J. Climate,* **11,** 1342–1355.

Kug. J.-S., Choi, J., An, S.-I., Jin, F.–F., Wittenberg, A.T., 2010: Warm pool and cold tongue El Niño events as simulated by the GFDL 2.1 coupled GCM. *J. Climate,* **23**, 1226–1239.

Latif, M., and co-authors, 2001: ENSIP: the El Niño simulation intercomparison project. *Clim. Dyn., **18***, 255–276.

Leloup, J., M. Lengaigne and J.-P. Boulanger 2008: Twentieth century ENSO characteristics in the IPCC database, *Clim. Dyn.,* **30,** 277-291.

Liang, J., X.-Q. Yang, D.-Z. Sun, 2012: The Effect of ENSO Events on the Tropical Pacific Mean Climate: Insights from an Analytical Model. *J. Climate*, in press.

Lu, P., J. P. McCreary Jr., and B. A. Klinger 1998: Meridional circulation cells and the source waters of the Pacific equatorial undercurrent, *J. Phys. Oceanogr.,* **28,** 62–84.

McPhaden, M.J, and co-authors, 1998: The Tropical Ocean-Global Atmosphere observing system: A decade of progress. *J. Geophys. Res.,* **103(C7),** 14,169-14,240

Mechoso, M. R., and Coauthors 1995: The seasonal cycle over the tropical Pacific in coupled ocean–atmosphere general circulation models, *Mon. Wea. Rev.,* **123,** 2825–2838.

460 Meehl, G.A., C. Covey, T. Delworth, M. Latif, B. McAvaney, J.F.B. Mitchell, R.J.
461 Stouffer and K.E. Taylor 2007: THE WCRP CMIP3 Multimodel Dataset: A New
462 Era in Climate Change Research, *BAMS*, **88,** 1383-1394, DOI:
463 10.1175/BAMS-88-9-1383.

464 Newell, R. E., 1979: Climate and the ocean. *Amer. Sci.*, **67**, 405–416.

465 Philander, S. G. 1990: El Niño, La Niña and the Southern Oscillation, 293 pp,
466 Elsevier, New York.

467 Pierrehumbert, R. T. 1995: Thermostats, radiator fins, and the runaway greenhouse, *J.*
468 *Atmos. Sci.,* **52,** 1784–1806.

469 Ramananthan, V. and W. Collins 1991: Thermodynamic regulation of ocean warming
470 by cirrus clouds deduced from observations of the 1987 El Niño. *Nature,* 27—32.

471 Rayner N. A., D. E. Parker, E. B. Horton, C. K. Folland, L. V. Alexander, D. P.
472 Rowell, E. C. Kent, and A. Kaplan 2003: Global analyses of sea surface
473 temperature, sea ice, and night marine air temperature since the late nineteenth
474 century, *J. Geophys. Res.,* **108,** 4407, doi:10.1029/2002JD002670.

475 Rodgers, K. B., P. Friederichs, and M. Latif 2004: Tropical Pacific decadal variability
476 and its relation to decadal modulation of ENSO, *J. Climate,* **17,** 3761–3774.

477 Rossow, W. B., and R. A. Schiffer 1999: Advances in understanding clouds from
478 ISCCP, *Bull. Amer. Meteor. Soc.,* **80,** 2261–2288.

479 Schopf, P. S., and R. J. Burgman 2006: A simple mechanism for ENSO residuals and
480 Asymmetry, *J. Climate,* **19,** 3167–3179.

481 Spencer, R. W. 1993: Global oceanic precipitation from the MSU during 1979-91 and
482 comparisons to other climatologies, *J. Climate,* **6,** 1301-1326.

483 Sun, D.-Z., and Z. Liu 1996: Dynamic ocean–atmosphere coupling: A thermostat for
484 the tropics, *Science,* **272,** 1148–1150.

485 Sun, D.-Z., and K. E. Trenberth 1998: Coordinated heat removal from the equatorial
486 Pacific during the 1986–87 El Niño, *Geophys. Res. Lett.,* **25,** 2659– 2662.

487 Sun, D.-Z. 2000: Global climate change and ENSO: a theoretical framework. In El
488 Niño: Historical and Paleoclimatic Aspects of the Southern Oscillation,
489 Multiscale variability and Global and Regional Impacts, 443-463. Edited by Diaz
490 H. F. and V. Markgraf, 476 pp, Cambridge University Press, Cambridge.

491 Sun, D.-Z. 2003: A possible effect of an increase in the warm-pool SST on the
492 magnitude of El Niño warming, *J. Climate,* **16,** 185– 205.

493 Sun, D.-Z. and T. Zhang 2006: A Regulatory Effect of ENSO of ENSO on the
494 Time-Mean Thermal Stratification of the Equatorial Upper Ocean, *Res. Lett.,* **33,**
495 L07710, doi:10.1029/2005GL025296.

Sun, D.-Z. 2007: The Role of ENSO in Regulating its Background State. in *Nonlinear Dynamics in Geosciences,* pages 537-555, Edited by J. Elsner and A. Tsonis, Springer New York.

Sun, D.-Z. 2010: The Diabatic and Nonlinear Aspects of El Niño-Southern Oscillation: implications for its past and Future Behavior, in Climate Dynamics: Why Does Climate Vary?, AGU Geophysical Monograph, Edited by D.-Z. Sun and F. Bryan, AGU.

Sun, F. P., J.-Y. Yu, 2009: A 10-15-yr modulation cycle of ENSO intensity. *J. Climate*, **22,** 1718-1735.

Trenberth, K. E., and A. Solomon 1994: The global heat balance: Heat transports in the atmosphere and ocean, *Clim. Dyn.,* **10,** 107–134.

Webster, P. J., and R. Lukas 1992: TOGA COARE: The Coupled Ocean-Atmosphere Response Experiment, *Bull. Am. Meteorol. Soc.,* **73,** 1377-1417.

Zhang, T., D.-Z. Sun, R. Neale, and P. Rasch 2009: An Evaluation of ENSO Asymmetry in the Community Climate System Models: A View from the Subsurface, *J. Climate,* doi: 10.1175/2009JCLI2933.1.

515 **Table Legends:**

516

517 Table 1: Color schemes used to denote the data from different models and
518 observations. The number of runs for each model and the origin of the countries of the
519 models used are also listed. The dominance of the U.S. in climate modeling is
520 apparent. Only models without the use of flux adjustment are included in this study.

521

Figure Legends:

Figure 1 (a): Probability density function (PDF, blue curve) for the climatological annual mean warm pool size. The red vertical line indicates the observed value and the blue vertical line indicates the averaged value of all model runs. The short colored marks on the horizontal axis indicate the values of individual runs in all models. (b): Time series for the western Pacific warm-pool size in observations (black) and 19 IPCC models (colors) over the last century. Shown in Fig.1b are the multi-run ensemble mean values smoothed by a cosine bell window with a width of of 49 months. The warm pool is defined as the region where SST is higher than 28ºC. Shown are the results using the data from 1950 to 1999 period, which are considered more reliable. The results based on the data over the entire 20th century are similar to those shown here. Color scheme for identifying models is provided in Table 1.

Figure 2: The climatology of 28ºC SST in the models (colors) and observations (black). Shown are results for the period 1950 to 1999. Only the results for the ensemble mean of the models are shown in the figure for clarity. Color scheme for identifying models is provided in Table 1.

Figure 3: Same as Fig. 2, but for all the runs of the same model--the NCAR CCSM3 (a) and GFDL CM2.1 (b). Note that the variability among the different runs is small in the same model, but the variability is signigicant between models and

observations.

Figure 4: (a) Same as Fig.1a, but for the mean warm-pool SST; (b) Same as Fig.1b, but for the mean warm-pool SST. (c) Same as Fig.1a, but for the Maximum SST, (d) Same as Fig.1b, but for the Maximum SST.

Figure 5: The probability density function (PDF) (blue curve) for the skewness of monthly Niño3 SST anomaly. Data used to construct this figure are the same as for Fig. 1a. The color scheme for indicating the models is also the same. The red vertical line indicates the value for observations. The vertical blue line is the multi-model ensemble mean. The short color bars on the horizontal axis mark the values for the individual runs in all the models.

Figure 6: The frequency distribution of monthly Niño3 SST anomaly. Data and color scheme used in this figure are the same as for Fig. 6. Only the ensemble mean of the models are drawn. Color scheme for identifying the models is provided in Table 1.

Figure 7: Same as Fig. 7, but for runs from a single model—the GFDL_CM2_0 (a), GFDL_CM2_1 (b), NCAR CCSM3 (c) and NCAR PCM1 (d).

Figure 8. (a) is the scatter plot between variance ($^{\circ}C^2$) and skewness of Niño3 SST anomaly from 1950 to 1999 and (b) is the scatter plot between mean western Pacific warm pool size (m^2) and skewness of Niño3 SST anomaly from 1950 to 1999. The black pentagram represents

the observation and the hexagram represents the average of all IPCC model runs. Colors and its data names refer to Table 1. Same model use the same color and the different markers in the same color represent the different runs in the same model.

Figure 9. The first EOF mode of the tropical pacific SST from 1950 to 1999 in observation (HadISST) and in IPCC Ar4 models. The first plot is for the observation and the rest are for models. Each model is the results of the multi-run ensemble mean. The SST anomaly in all plots use the same color scale.

Figure 10. (a) is the PDF analysis of the skewness of the time series in 1 EOF mode in observation and in model ensemble means. The red vertical line indicates the value for observations. The vertical blue line is the multi-model ensemble mean. The short color bars on the horizontal axis mark the multi-run ensemble mean values for the individual models. (b) is the scatter plot between mean western Pacific warm pool size (m^2) and skewness of time series of first EOF mode in models and in observation from 1950 to 1999. The black pentagram represents the observation and the hexagram represents the average of all IPCC model ensemble means. Colors and its model names refer to Table 1.

Figure 11. The residual time mean effect of ENSO due to ENSO asymmetry from 1950 to 1999. The residual effect is calculated by the mean SST anomaly in El Niño plus the mean SST anomaly in La Niña. The contours in red (black) represent the 28°C mean SST during El Niño (La Niña). The El Niño (La Niña) is based on a threshold of +(-) 0.5°C for the Niño 3 region (5°N-5°S, 150°-270°W). Numbers and its data name are listed in Table 1. The two models (BCCR-BCM2-0 and CNRM-CM3) with too small or no warm-pool and three models (GISS-AOM, GISS-MODEL-E-H and GISS-MODEL-E-R) with no ENSO are removed from the plots.

Figure 12. a, c, e are the distribution for the Niño4, Niño3.4 and Niño3 index from 1950 to 1999. b, d, f are the probability density function for skewness of Niño4, Niño3.4 and Niño3 index from 1950 to 1999 respectively.

Figure 13. Scatter plot between the biases of warm pool simulation (western Pacific warm pool size, mean SST over western Pacific warm pool and maximum SST over western Pacific warm pool) and the biases of Niño index (Niño4, Niño34 and Niño3). The black hexagram represents the average of all IPCC model runs. Colors and its data names refer to Table 1. Same model use the same color and the different markers in the same color represent the different runs

in the same model. The Correlation coefficient (r) is calculated just base on the models located in the same quadrant with the pentagrams.

No.	Data Name	Country	Runs	Color
1	Observations			
2	BCCR-BCM2.0	Norway	1	
3	CNRM-CM3	France	1	
4	CSIRO-Mk3.0	Australia	3	
5	CSIRO-Mk3.5	Australia	3	
6	GFDL-CM2.0	United States	3	
7	GFDL-CM2.1	United States	5	
8	GISS-AOM	United States	2	
9	GISS-EH	United States	5	
10	GISS-ER	United States	9	
11	IAP-FGOALS-g1.0	China	3	
12	INGV-ECHAM4	Italy	1	
13	IPSL-CM4	France	1	
14	MIROC3.2-Hires	Japan	1	
15	MIROC3.2-Medres	Japan	3	
16	MPI-ECHAM5	Germany	3	
17	NCAR-CCSM3.0	United States	2	
18	NCAR-PCM1	United States	3	
19	UKMO-HadCM3	United Kingdom	2	
20	UKMO-HadGEM1	United Kingdom	2	

Table 1: Color schemes used to denote the data from different models and observations. The number of runs for each model and origin of the countries of the models used are also listed. The dominance of the U.S. in climate modeling is apparent. Most of the models, including those of the U.S., have a very modest number of runs. Note that only models without the use of flux adjustment are included in this study.

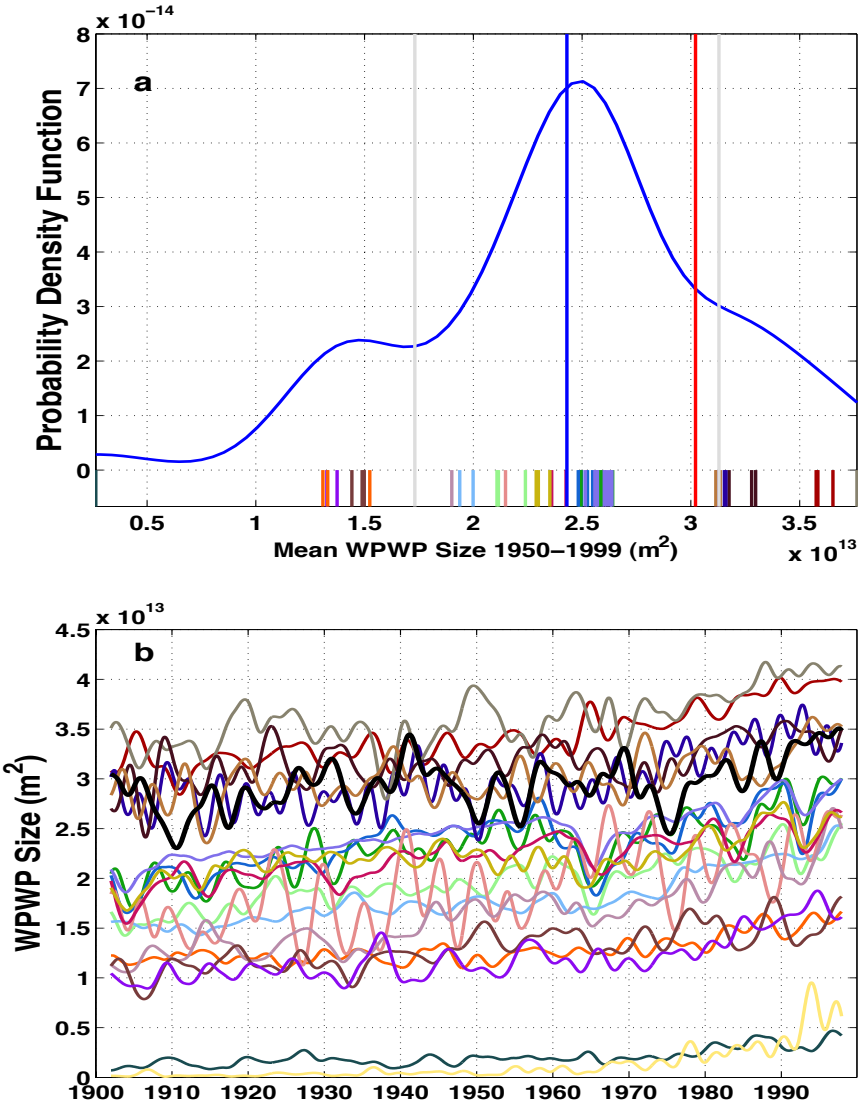

Figure 1 (a): Probability density function (PDF, blue curve) for the climatological annual mean warm pool size. The red vertical line indicates the observed value and the blue vertical line indicates the averaged value of all model runs. The short colored marks on the horizontal axis indicate the values of individual runs in all models. (b): Time series for the western Pacific warm-pool size in observations (black) and 19 IPCC models (colors) over the last century. Shown in Fig.1b are the multi-run ensemble mean values smoothed by a cosine bell window with a width of of 49 months. The warm pool is defined as the region where SST is higher than 28ºC. Shown are the results using the data from 1950 to 1999 period, which are considered more reliable. The results based on the data over the entire 20th century are similar to those shown here. Color scheme for identifying models is provided in Table 1.

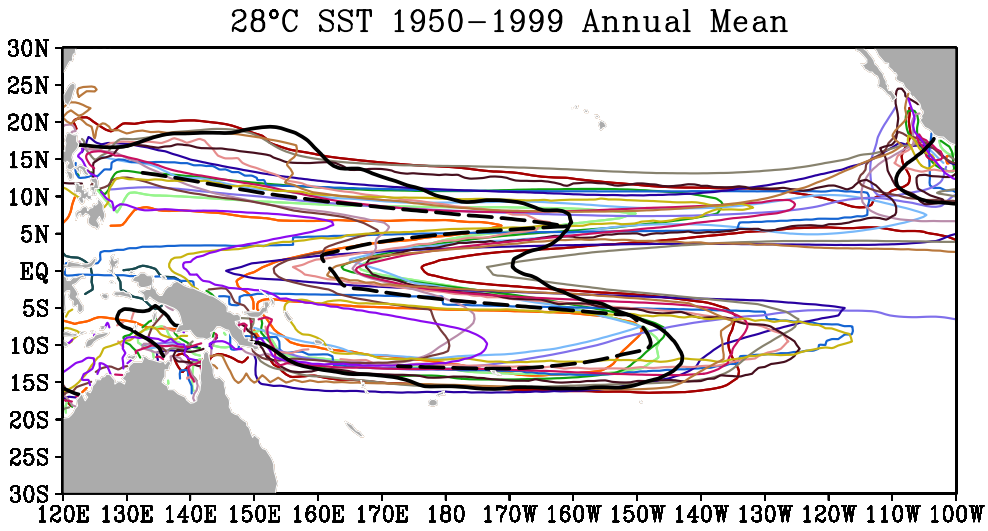

Figure 2: The climatology of 28ºC SST in the models (colors) and observations (black). Shown are results for the period 1950 to 1999. Only the results for the ensemble mean of the models are shown in the figure for clarity. Color scheme for identifying models is provided in Table 1.

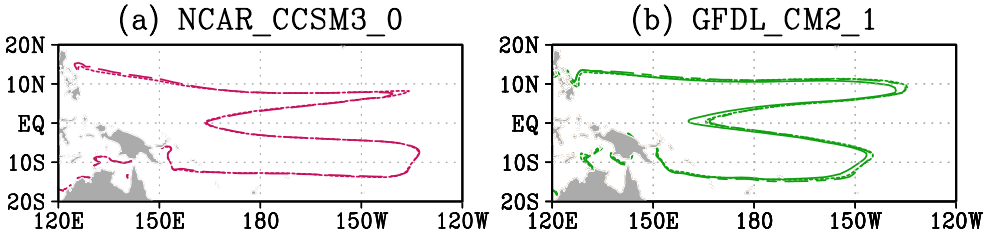

Figure 3: Same as Fig. 2, but for all the runs of the same model--the NCAR CCSM3 (a) and GFDL CM2.1 (b). Note that the variability among the different runs is small in the same model, but the variability is significant between models and observations.

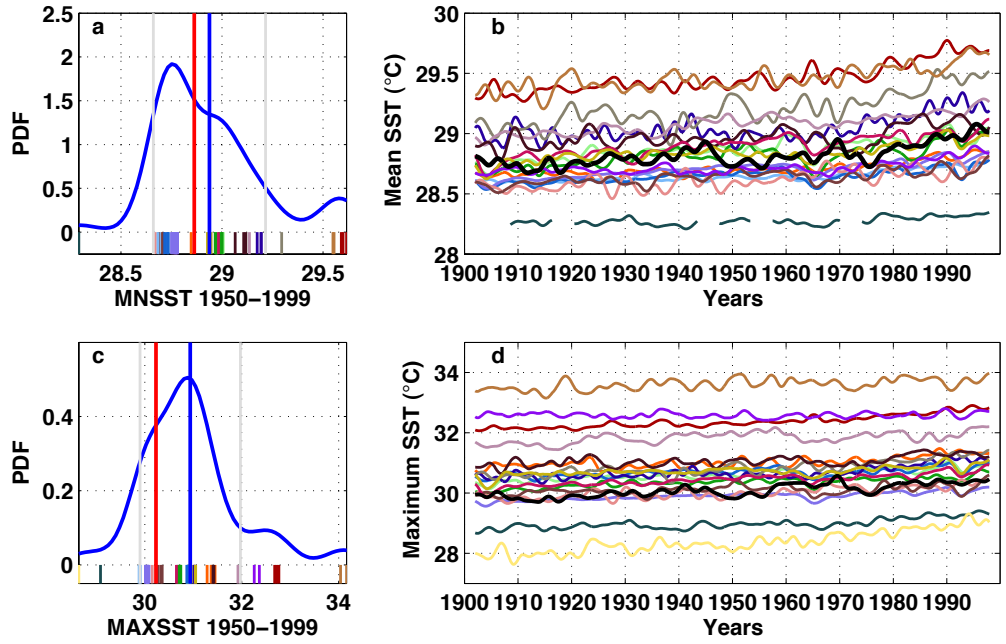

647

648 Figure 4: (a) Same as Fig.1a, but for the mean warm-pool SST; (b) Same as Fig.1b,
649 but for the mean warm-pool SST. (c) Same as Fig.1a, but for the Maximum SST, (d)
650 Same as Fig.1b, but for the Maximum SST.

651

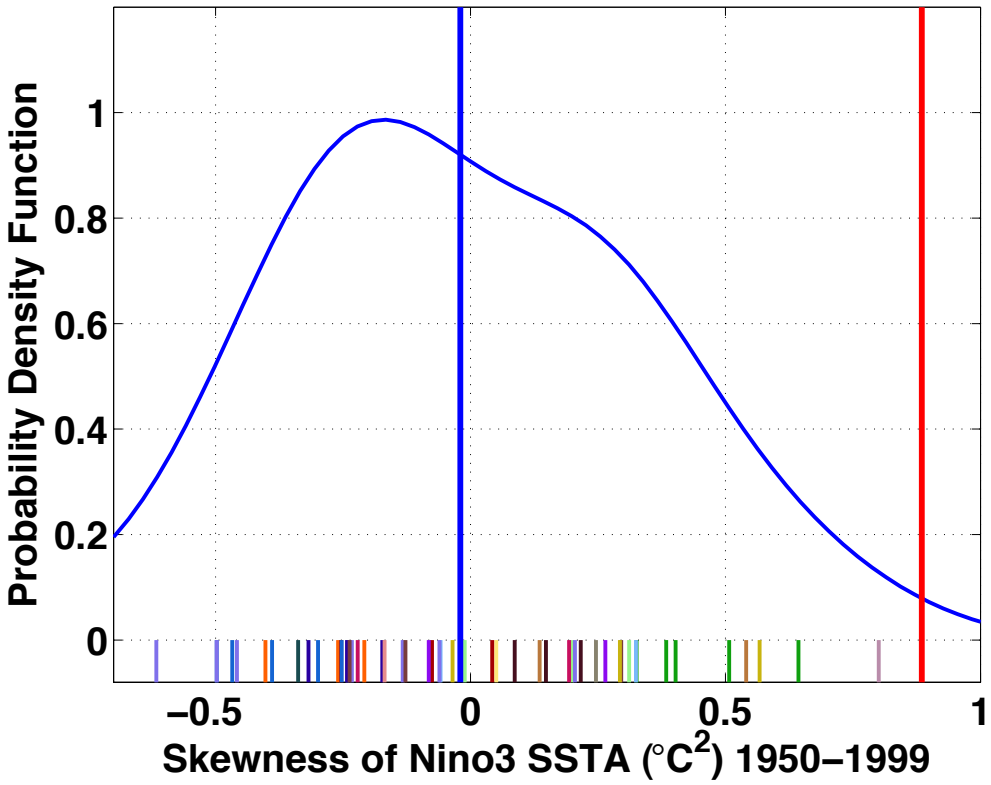

652

653 Figure 5: The probability density function (PDF) (blue curve) for the skewness of
654 monthly Niño3 SST anomaly. Data used to construct this figure are the same as for
655 Fig. 1a. The color scheme for indicating the models is also the same. The red vertical
656 line indicates the value for observations. The vertical blue line is the multi-model
657 ensemble mean. The short color bars on the horizontal axis mark the values for the
658 individual runs in all the models.

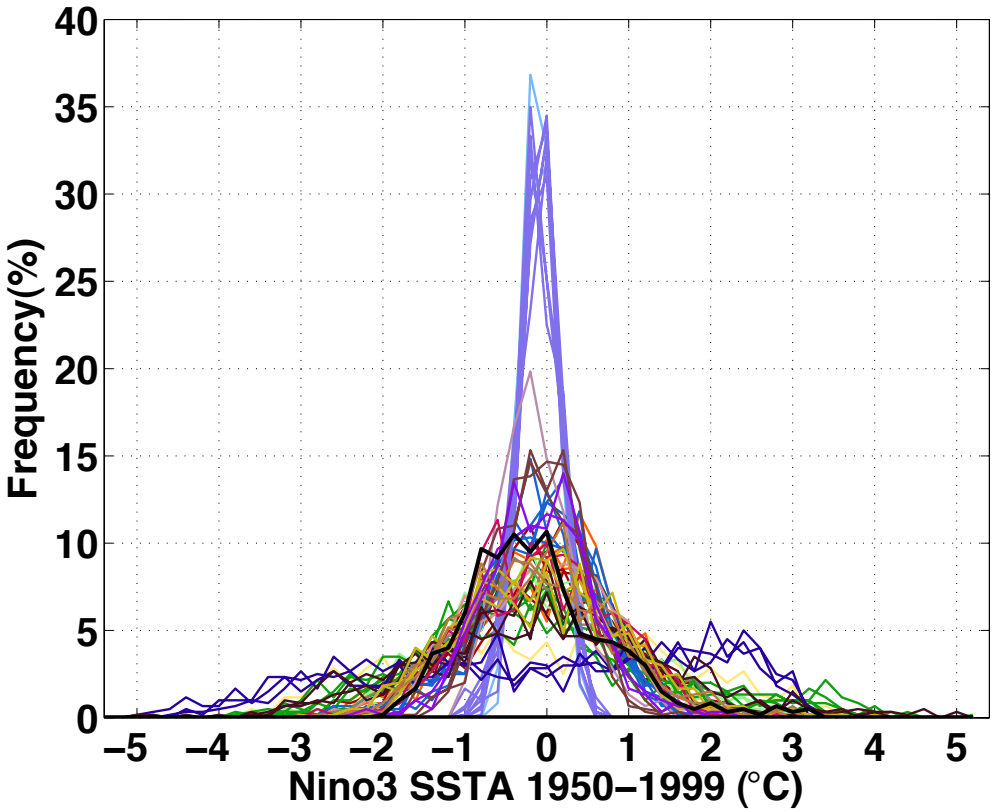

Figure 6: The frequency distribution of monthly Niño3 SST anomaly. Data and color scheme used in this figure are the same as for Fig. 6. Only the ensemble mean of the models are drawn. Color scheme for identifying the models is provided in Table 1.

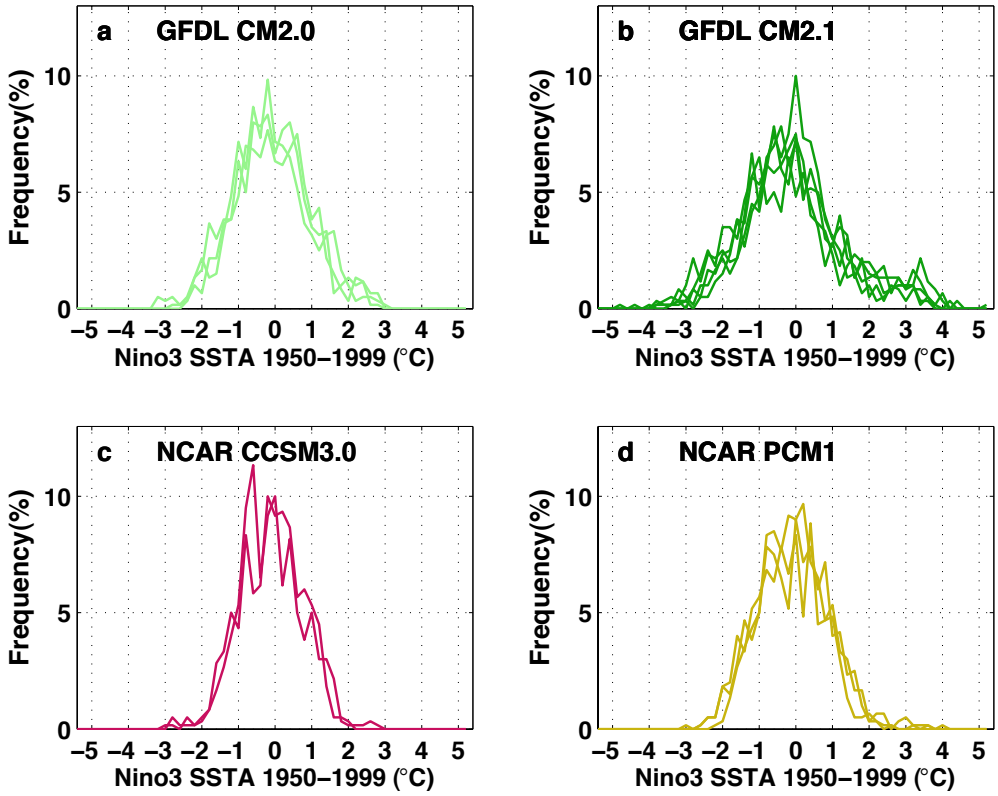

Figure 7: Same as Fig. 7, but for runs from a single model—the GFDL_CM2_0 (a), GFDL_CM2_1 (b), NCAR CCSM3 (c) and NCAR PCM1 (d).

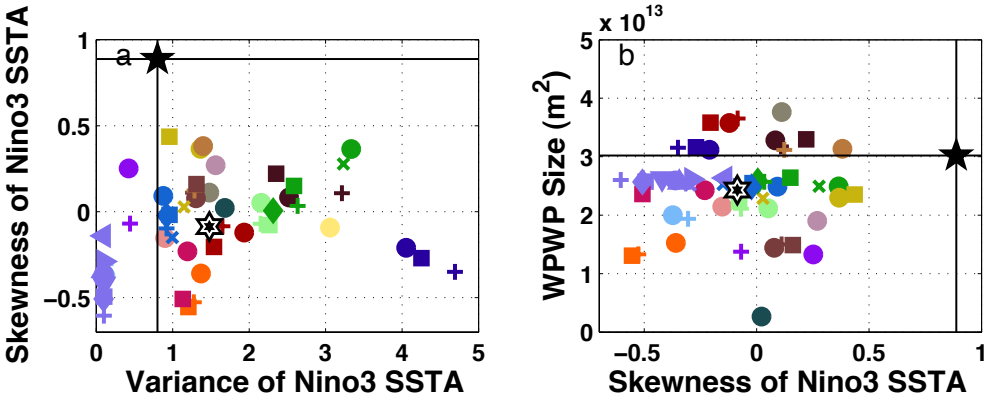

694

695 Figure 8. (a) is the scatter plot between variance ($^oC^2$) and skewness of Niño3 SST
696 anomaly from 1950 to 1999 and (b) is the scatter plot between mean western Pacific
697 warm pool size (m^2) and skewness of Niño3 SST anomaly from 1950 to 1999.The
698 black pentagram represents the observation and the hexagram represents the average
699 of all IPCC model runs. Colors and its data names refer to Table 1. Same model use
700 the same color and the different markers in the same color represent the different runs
701 in the same model.

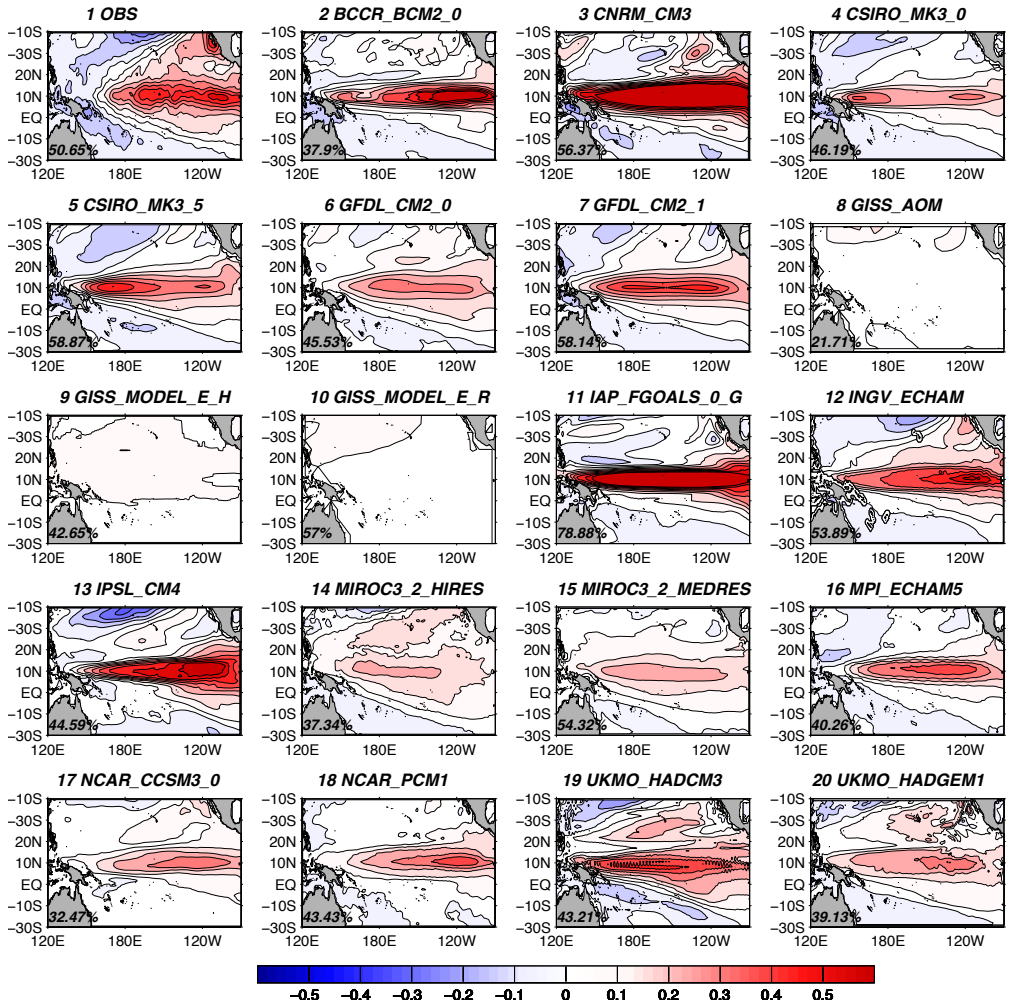

Figure 9. The first EOF mode of the tropical pacific SST from 1950 to 1999 in observation (HadISST) and in IPCC Ar4 models. The first plot is for the observation and the rest are for models. Each model is the result of the multi-run ensemble mean. The SST anomaly in all plots use the same color scale.

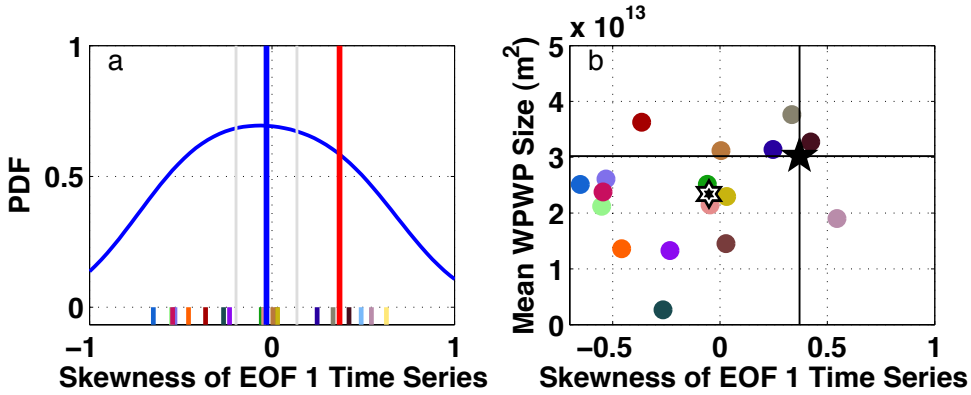

Figure 10. (a) is the PDF analysis of the skewness of the time series in 1 EOF mode in observation and in model ensemble means. The red vertical line indicates the value for observations. The vertical blue line is the multi-model ensemble mean. The short color bars on the horizontal axis mark the multi-run ensemble mean values for the individual models.(b) is the scatter plot between mean western Pacific warm pool size (m^2) and skewness of time series of first EOF mode in models and in observation from 1950 to 1999. The black pentagram represents the observation and the hexagram represents the average of all IPCC model ensemble means. Colors and its model names refer to Table 1.

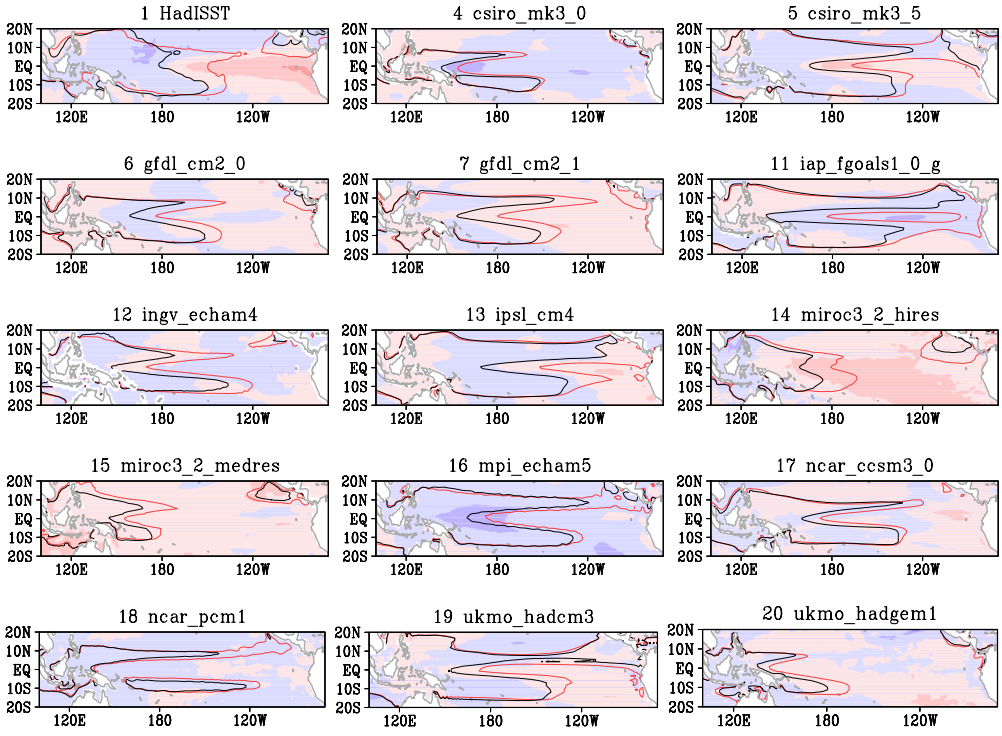

Figure 11. The residual time mean effect of ENSO due to ENSO asymmetry. The residual effect is calculated by the mean SST anomaly in El Niño plus the mean SST anomaly in La Niña. The contours in red (black) represent the 28ºC mean SST during

El Niño (La Niña). The El Niño (La Niña) is based on a threshold of +(-) 0.5°C for the Niño 3 region (5°N-5°S, 150°-270°W). Numbers and its data names are listed in Table 1. The two models (BCCR-BCM2-0 and CNRM-CM3) with too small or no warm-pool and three models (GISS-AOM, GISS-MODEL-E-H and GISS-MODEL-E-R) with no ENSO are removed from the plots.

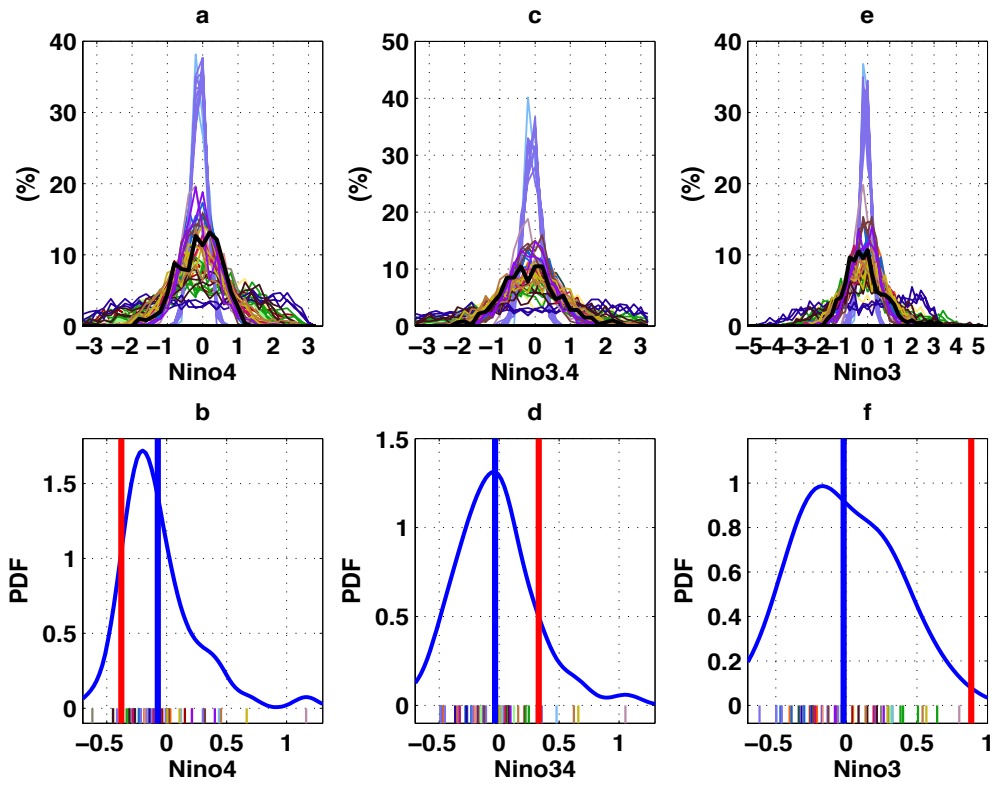

Figure 12. a,c,e are the distribution for the Niño4, Niño3.4 and Niño3 index from 1950 to 1999. b,d,f are the probability density function for skewness of Niño4, Niño3.4 and Niño3 index from 1950 to 1999 respectively.

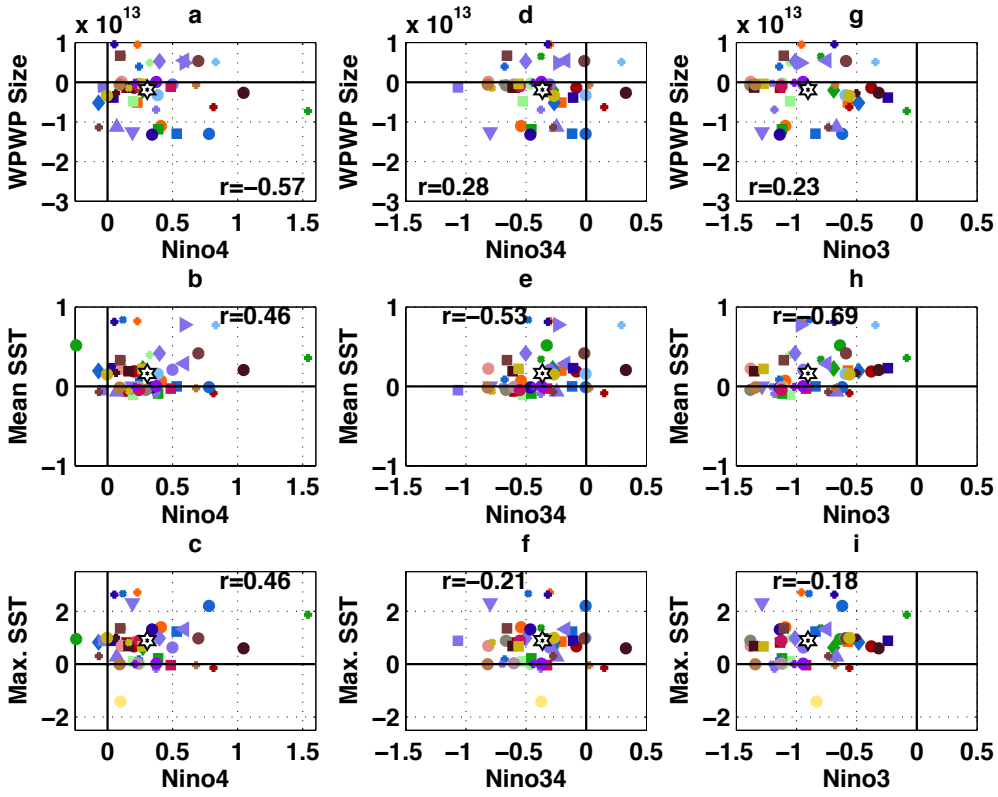

Figure 13. Scatter plot between the biases of warm pool simulation (western Pacific warm pool size, mean SST over western Pacific warm pool and maximum SST over western Pacific warm pool) and the biases of Niño index (Niño4, Niño34 and Niño3). The black hexagram represents the average of all IPCC model runs. Colors and its data names refer to Table 1. Same model use the same color and the different markers in the same color represent the different runs in the same model.
The Correlation coefficient (r) is calculated just base on the models located in the same quadrant with the pentagrams.